

RAPID-LLM: Resilience-Aware Performance analysis of Infrastructure for Distributed LLM Training and Inference

George Karfakis, Faraz Tahmasebi, Binglu Chen, Lime Yao, Saptarshi Mitra, Tianyue Pan, Hyoukjun Kwon, Puneet Gupta

Abstract

RAPID-LLM is a unified performance modeling framework for large language model (LLM) training and inference on GPU clusters. It couples a DeepFlow-based frontend that generates hardware-aware, operator-level Chakra execution traces from an abstract LLM specification (model shape, batch/sequence settings, training vs. inference, and hybrid parallelism choices) with an extended Astra-Sim backend that executes those traces on explicit multi-dimensional network topologies with congestion-aware routing and support for degraded and faulty links. The frontend assigns per-operator latency using a tile-based model that accounts for SM under-utilization and multi-level memory traffic (SRAM/L2/HBM), and prunes memory-infeasible configurations using an activation-liveness traversal under recompilation, parallelism and ZeRO/FDSP sharding policies.

Across A100-based validation cases, RAPID-LLM predicts Llama inference step latency and GPT-scale training time per batch within 10.4% relative to published measurements, and matches ns-3 packet-level results within 8% on representative communication workloads. Case studies demonstrate how RAPID-LLM enables fast, exhaustive sweeps over hybrid-parallel configurations, quantifies sensitivity to soft link faults under realistic routing and congestion, and evaluates hypothetical GPU design variants including HBM bandwidth throttling effects.

1 Introduction

Today’s large language models (LLMs) are trained and served on clusters of GPU-based systems comprising hundreds to thousands of nodes. Training runs are long and communication heavy, while inference workloads push for high throughput and tight latency. In both phases, end-to-end performance emerges from coupled interactions between GPU microarchitecture, the memory hierarchy, and the surrounding interconnect fabric. As deployments grow in scale and complexity, it becomes increasingly difficult to predict how changes in networking, workload structure and hardware design will affect training time, inference latency, and overall resource efficiency.

To explore future systems, practitioners increasingly turn to modeling tools that predict end-to-end LLM training and

inference behavior using configurable abstractions. Symbolic or analytic workload descriptions coupled to network simulators (e.g., AstraSim and STAGE [21, 33]) can represent large distributed jobs and a variety of topologies, but they often reduce compute and memory models to coarse layer-level models. Trace-driven tools (e.g., SimAI and ReaLLM [26, 32]) ingest measurements from real runs and achieve high realism for the profiled hardware and network, but they are tied to that deployment. Detailed GPU or multi-GPU simulators (e.g., Accel-Sim and GPGPU-Sim [3, 15]) can model fine-grained behavior, but their high runtime confines them to smaller systems and fewer design points rather than cluster-scale, forward-looking exploration.

To address these limitations, a useful modeling framework must bridge hardware detail and cluster-scale scope. It should capture operator-level compute, cache and memory interactions, and realistic interconnect dynamics, while scaling to large systems and running fast enough to explore many scenarios. It should support both training and inference on a shared hardware description across common LLM parallelization strategies and explicitly model link faults and routing-dependent congestion. To enable future-facing design space exploration, it should accept abstract specifications of GPUs, memory stacks, packaging, and network topologies instead of traces from a specific deployment.

RAPID-LLM is designed to meet these requirements by coupling a DeepFlow-based frontend, which generates synthetic hardware-informed, operator-level execution traces from abstract LLM training and inference configurations, with an extended AstraSim-based back end that executes those traces on realistic, fault- and congestion-aware multi-dimensional networks. Together, these components capture the coupled behavior of compute, memory, and communication, while remaining scalable and fast enough to explore many hardware and network scenarios.

Two simple examples illustrate why these properties matter. Consider a large LLM training job that uses pipeline parallelism across many GPUs. A single faulty, degraded inter-node link can have very different impact on end-to-end throughput depending on its position: in one layout, it lies on a critical cut and stalls the pipeline, while in another most traffic bypasses it and throughput changes little. Unlike

prior tools, RAPID-LLM distinguishes these outcomes as it considers topology, routing, and time-varying congestion, not just average per-link bandwidth.

As a second example, consider the attention operator in a transformer block. Compared to a naive implementation, FlashAttention[6] performs similar arithmetic but exercises the memory hierarchy very differently, as it keeps working set tiles resident in fast on-chip memory. In contrast, naive attention streams full intermediate tensors from external memory. On real GPUs, these data-movement differences often dominate runtime [6], so any tool that only counts flops or uses layer-level bandwidth models will mispredict their relative performance as well as sensitivity to cache sizes and memory bandwidth. RAPID-LLM avoids this pitfall by constructing hardware-aware traces that consider a multi-level tiling and memory hierarchy.

This paper makes the following contributions:

1. We extend DeepFlow to produce hardware-aware per-operator Chakra execution traces for LLM training and inference under hybrid parallelism strategies.
2. We extend AstraSim with multi-dimensional congestion-aware routing and modeling of degraded and faulty links, enabling realistic large-scale network simulation across diverse topologies and fault patterns.
3. We use these components to build RAPID-LLM, a highly scalable and unified modeling framework, validate it against real deployment measurements with comparisons to representative existing tools, and conduct case studies analyzing packaging, memory configurations, and the impact of link faults and mapping decisions.

The remainder of this paper is organized as follows. Section 2 formalizes the problem and reviews background on LLM workloads. Section 3 reviews existing approaches and motivates the need for a more robust unified modeling framework. Section 4 describes the design of RAPID-LLM, including its constituent components and their extensions. Section 5 presents our validation methodology and comparative evaluation. Section 6 presents case studies that visit hardware and network what-if scenarios that are uniquely enabled by RAPID-LLM. Section 7 concludes with a discussion of limitations and directions for future work.

2 Background

Modern LLM deployment on server-class clusters. As LLMs scale to trillions of parameters, training and inference increasingly rely on datacenter-scale GPU clusters. For example, Llama 3 405B was trained on 16,384 H100 GPUs with a reported Model FLOPs Utilization (MFU) of only $\approx 38\%$ [8]. At this scale, throughput is often limited less by raw compute than by memory capacity and communication: parameters, activations, optimizer state, and inference-time KV caches dominate device memory usage, stressing HBM

Table 1. Dominant communication patterns for common parallelism types during FP & BP in large-scale LLM training. Patterns follow common Megatron-style[30] configurations and are indicative only. Abbreviations: AG = AllGather, AR = AllReduce, RS = ReduceScatter, A2A = AllToAll, P2P = point-to-point send/recv, blk = structured block exchange.

Parallelism	FP	BP
Data (DP)	–	AR
Tensor / model (TP)	AG / AR	AR
Pipeline (PP)	P2P	P2P
Sequence (SP)	AG / RS	AG / RS
Context (CP)	A2A / blk	A2A / blk

capacity and increasing communication pressure [2, 18, 27]. How this state is partitioned and communicated directly shapes training throughput and inference latency.

These trends motivate hybrid parallelism strategies and the need for models that capture the interaction between compute, memory, and communication on large GPU clusters.

Parallelism strategies in distributed LLMs. We focus on five spatial parallelism axes used in large-scale LLM systems:

- **Data parallelism (DP)** replicates the model across workers and shards the input batch across replicas.
- **Tensor/model parallelism (TP)** partitions individual layers across devices so that each GPU holds only a shard of the weights and activations[30].
- **Pipeline parallelism (PP)** partitions the layer stack into stages mapped to different GPUs, with microbatches flowing across stages[13].
- **Sequence parallelism (SP)** shards intermediate activations along the sequence dimension and synchronizes around sequence-wide operations[16].
- **Context parallelism (CP)** assigns different token ranges to different GPU groups and exchanges attention KV tensors between them before attention[20].

In practice, production deployments use hybrid parallelism. For example, the final stage of Llama 3 405B pre-training runs on 16,384 GPUs with TP=8, CP=16, PP=16, and DP=8 to support 131k-token sequences [8], creating overlapping collective and point-to-point communication. Training consists of a forward pass (FP) and a backward pass (BP), with BP covering both activation and weight gradients, while inference (prefill and decode) largely reuses FP communication patterns. Table 1 summarizes the dominant communication patterns introduced by each parallelism axis during FP and BP in Megatron-style implementations [30].

Cluster interconnects and topologies. Modern GPU clusters expose a multi-level communication hierarchy: GPUs

within a node are connected by high-bandwidth, low-latency fabrics such as NVLink and NVSwitch, while inter-node communication relies on InfiniBand or RDMA-capable Ethernet [19, 22–24]. Logically, the cluster forms a multi-dimensional network spanning intra-node, intra-rack/pod, and inter-rack/pod dimensions.

At the network level, links are organized into switch-centric Fat-Tree/Clos or direct-connect mesh and torus topologies [1, 5]. Collective operations generate heavy traffic on these fabrics, creating congestion that depends on the mapping of parallelism groups to the physical topology. Realistic performance models must therefore capture the hierarchical structure of links, multi-dimensional contention, and routing-dependent effective bandwidth.

Faults and degraded links at scale. Hardware and network instability are a constant reality at LLM-training scale [9]. For instance, Meta reports over 400 unexpected job interruptions during Llama 3 training on a 16k-GPU cluster [8], with nearly half attributed to hardware or infrastructure failures. More subtle are link-level problems: persistent bandwidth degradation or elevated error rates that cause retransmissions [10], which reduce the effective capacity of specific routes [12].

Hybrid parallelism creates tightly coupled communication patterns across many GPUs, so such link-level anomalies on a critical cut can materially reduce effective system performance. Models that assume fully healthy links and static per-link bandwidth cannot capture these effects. Accurately reasoning about performance therefore requires congestion-aware network models that can represent both contention and explicit link faults.

3 Existing approaches/related work

Prior work on modeling and simulation for large-scale LLM training and inference spans a wide spectrum of fidelity and scalability. Most systems can be understood as composing a compute frontend that produces a time-ordered stream (or dependency graph) of compute and communication events, and a network/backend model that predicts the cost of those communication events under a chosen topology and contention model, sometimes with a similarly abstract compute backend. We adopt this decomposition to separate what existing tools can represent about LLM workloads from what they can realistically predict about cluster-scale execution.

Compute frontend models. Compute frontends for LLM training and inference broadly fall into three categories: (1) trace-driven profiling and replay, (2) cycle(-approximate) accelerator simulators, and (3) analytical node-level models.

Trace-driven tools extrapolate execution profiles from real runs, offering high realism but limited ability to explore future hardware and network designs due to their reliance

on system-specific measurements. Examples include SimAI [32] and Chakra- or ReaLLM-style trace replay [26, 31].

Cycle-level simulators provide detailed modeling of accelerator internals, such as GPGPU-Sim and Accel-Sim for GPUs [3, 15] and ONNXim for NPUs [11], but their high cost limits scalability to cluster-scale LLM studies.

Analytical node-level models use FLOP- and tensor-size-based roofline estimates; MLSynth [29] and STAGE [21] follow this approach. However, coarse global scaling reduces accuracy when performance depends on operator shape or memory hierarchy effects. Our frontend remains analytical but incorporates operator-level, hardware-aware memory modeling to bridge roofline models and trace realism.

Network backend models. Given a stream of communication events from a compute frontend, modeling tools typically rely on one of three network backends: simple analytic models, packet-level simulators, or analytical topology- and congestion-aware models. Astra-Sim [33] exposes all three as swappable backends, a pattern also seen in end-to-end tools.

Simple analytic backends estimate communication time from message size, bandwidth, and latency, and are fast but unable to capture congestion or link-level effects (e.g., ReaLLM [26], Astra-Sim’s congestion-unaware backend).

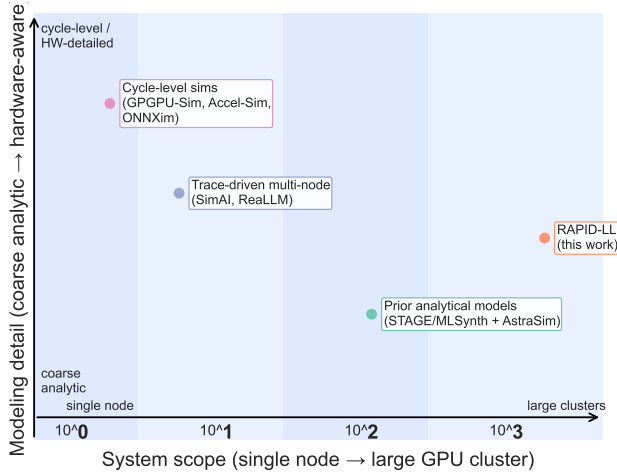
At the other extreme, packet-level simulators such as ns-3 [28] provide high-fidelity modeling of arbitrary topologies and congestion, but are prohibitively slow for cluster-scale LLM studies.

Between these extremes, analytical congestion-aware backends explicitly model links and contention; Astra-Sim’s representative backend, however, supports only a single logical dimension and assumes homogeneous, healthy links.

Overall, existing backends either miss multi-dimensional congestion, assume uniform link health, or are too slow for design-space exploration. Our backend extends Astra-Sim’s congestion-aware approach to multi-dimensional topologies with explicit links, capturing contention and degraded or faulty links at analytical cost.

Problem statement and modeling requirements. The discussion above points to a missing regime: we need a tool that can generate future-facing execution traces for both LLM training and inference from abstract model and hardware descriptions, and can model realistic multi-dimensional fabrics with congestion and link faults at analytical cost. Concretely, such a tool must combine operator-level, hardware-aware compute modeling (including memory hierarchy effects) with an analytical network model that instantiates links, captures multi-dimensional contention, and represents both degraded and failed links and scales to realistic thousand-GPU scenarios. A qualitative positioning of RAPID-LLM is shown in Figure 1, and a comparative comparison with other similar tools is shown in table 2.

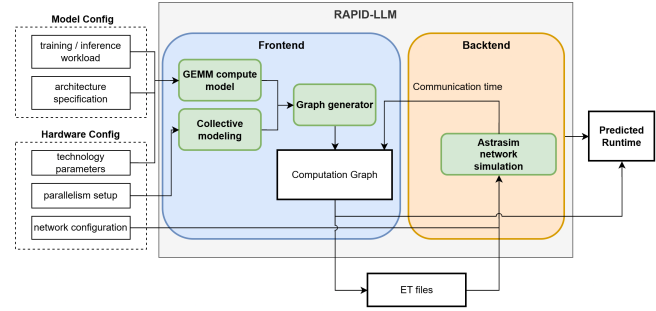
Comparison point	RAPID-LLM	STAGE + Astra-Sim[21, 33]	MLSynth + Astra-Sim[29, 33]	LLMCompass[34]	LLMServingSim[4]	ReaLLM[26]
Training / inference modeling	Both	Training only	Training only	Inference only	Inference only	Inference only
Advanced LLM modeling (ZeRO 1/2/3 DP, recompute, flash attention, etc.)	Yes	Yes	No	Yes	No	No
Compute model hardware awareness	Advanced (tiling, dtypes, fusion)	Basic Roofline	Basic Roofline	Advanced	Basic Roofline	Basic Roofline
Memory hierarchy modeling	Advanced (HBM/L2/DRAM)	None	None	Basic (tile-level only)	None	None
Network modeling	ASTRA-sim (extended)	ASTRA-sim (stock)	ASTRA-sim (stock)	Analytical, no congestion model	ASTRA-sim (stock)	Analytical, no congestion model
Network congestion modeling	Extended	Stock	Stock	None	Stock	None
Multi-dimension network fabrics	Yes	Limited	Limited	No	Limited	No
Link errors / retries impact	Yes	No	No	No	No	No

Table 2. High-level capability comparison across tools.**Figure 1.** Qualitative positioning of LLM modeling tools along modeling detail and system scope. RAPID-LLM targets a regime of operator-level, hardware-aware modeling at cluster scale.

The next section describes its architecture and components.

4 RAPID-LLM

Figure 2 shows the overall RAPID-LLM workflow. Each simulation run takes two inputs: an LLM workload specification (model architecture, training or inference request, and parallelism configuration) and a hardware specification (per-device parameters, cluster topology, and optional link faults). The frontend consumes these inputs to build an operator-level computation graph with explicit compute and communication tasks, then emits per-GPU Chakra execution traces. The backend executes these traces on an extended Astra-Sim network model with multi-dimensional congestion and fault awareness, producing end-to-end runtime estimates

**Figure 2.** Overview of RAPID-LLM

and compute/communication breakdowns for both training and inference.

4.1 Frontend: workload specification and trace generation

The RAPID-LLM frontend transforms high-level LLM and hardware specifications into an operator-level computation graph and per-GPU Chakra execution traces that drive the network backend.

Workload and hardware specification. RAPID-LLM builds on DeepFlow[25], extending it from LSTM-based models to modern decoder-only LLMs. Models are described by parameters such as number of layers, hidden dimension, number of attention heads, vocabulary size, and sequence lengths, in addition to training or inference specific hyper-parameters such as prefill/decode length and batch size. The deployment is described by a hardware specification (per-GPU compute and memory parameters) and a hybrid parallelism configuration that sets the degrees of DP, PP, CP and TP and maps them onto the available GPUs. Given these inputs, the frontend synthesizes a per-GPU workload that assigns each operator to a device according to the chosen parallelism strategy.

Operator-level performance modeling. The hardware-aware compute model then assigns times to each operator. Attention/FeedForward GEMM shapes reflect the underlying LLM and parallelism configuration (e.g., large prefill GEMMs, skinny decode GEMMs, per-head projections), and their latency is set via searching over a set of candidate tiling strategies. For each candidate, it estimates SM occupancy and the number of execution “waves” to account for under-utilization when the grid does not map onto the SMs, and derives SRAM/L2/HBM traffic from the tile sizes and tensor dimensions. When modeling L2 as a cache, we estimate miss rates with a lightweight reuse analysis to account for thrashing-driven increases in HBM traffic. This traffic is mapped onto a multi-level roofline model built from the provided peak throughput and bandwidths at each memory level, with the compute roofline derated based on the predicted occupancy and wave count. This allows the model to capture detailed, hardware-aware compute-bound and memory-bound regimes without full microarchitectural simulation. Pointwise and reduction operators (e.g., Softmax) are modeled with a simpler analytical bandwidth model that captures their arithmetic intensity and memory usage, and fused kernels such as FlashAttention[6] are treated as composite operators with adjusted tiling and memory access patterns to reflect reduced off-chip traffic. Communication operators are represented as nodes with a noted collective type (e.g, All-Reduce), total bytes, and participating ranks. These linearized graphs are then fed into the network backend.

Computation graph and Chakra traces. Given per-operator costs and placements, RAPID-LLM constructs a computation graph whose nodes correspond to compute and communication tasks and whose edges encode data and synchronization dependencies. The graph reflects the chosen hybrid parallelism configuration, with tensor and sequence/context parallelism sharding intra-layer operators across GPUs and pipeline and data parallelism introducing cross-layer and cross-microbatch dependencies. The frontend then linearizes this graph into per-GPU Chakra [31] execution traces that record, for each device, the ordered sequence of compute and communication events and their intra- and inter-device dependencies. Inter-device dependencies are modeled as Point-To-Point communication control nodes.

Memory modeling. RAPID-LLM also checks whether a given configuration fits in device memory. For each GPU, the frontend first estimates static memory usage for parameters, optimizer state, gradients, and (for inference) KV caches under the chosen parallelism, precision (mixed vs FP32) and ZeRO[27] (stages 1,2,3) sharding settings. It then performs a simulated traversal of the computation graph under a specified recomputation policy (full vs selective [6, 16]), tracking live activations over time and recording the peak activation

footprint per GPU for the given hybrid parallelism configuration. It then prunes configurations that exceed the total memory capacity of the GPU, allowing subsequent performance studies to focus on memory-feasible designs.

4.2 Backend: network modeling

RAPID-LLM executes Chakra [31] execution traces on an extended version of Astra-Sim’s congestion-aware analytical backend[33]. The backend constructs explicit multi-dimensional topologies, models congestion on a per-link basis, and supports soft and hard fault in links, while providing an extended library of base topologies and collective algorithms.

Multi-dimensional topology construction and congestion. In contrast to distance-based multi-dimensional abstractions utilized by congestion-unaware tools, RAPID-LLM’s backend instantiates all links in each dimension of the network. Users describe an N -dimensional fabric by selecting a base topology and node count for each dimension (e.g., [Ring, Ring] with [4,4] nodes for a 4x4 Torus topology), and the backend recursively builds the corresponding structure. Compared to the simpler networking topology library of AstraSim, RAPID-LLM’s backend supports topologies such as N -D Mesh, Torus, KingMesh, and HyperCube are supported as first-class building blocks. For each link, the backend tracks queues and simulates collective and point-to-point operations over the full multi-dimensional fabric, enabling congestion-aware modeling across dimensions rather than relying on hop-count approximations. Figure 3 summarizes the topology structures currently supported by RAPID-LLM.

As communication events from Chakra traces traverse the network, the backend records how many flows share each link and accounts for queueing and congestion delays when links are oversubscribed. Figure 4 illustrates an example where multiple flows contend for a subset of links in a multi-dimensional topology and RAPID-LLM captures the resulting congestion and delay.

Fault-aware network modeling. RAPID-LLM’s backend models both soft faults, where a link remains usable but at reduced effective bandwidth or higher latency (e.g., due to retries), and hard faults, where a link is removed from the topology. Given a fault configuration (pairs of endpoints and fault rates), the backend adjusts per-link bandwidth, and routes collectives using fault-aware variants of dimension-order routing that avoid unusable links when possible. Traffic rerouted around faults may break symmetry and can create new congestion hotspots that the our backend captures. Figure 5 shows two examples where hard faults force traffic onto alternate paths and induce additional congestion.

4.3 Execution modes & Scalability

RAPID-LLM can execute LLM workloads in two separate modes:

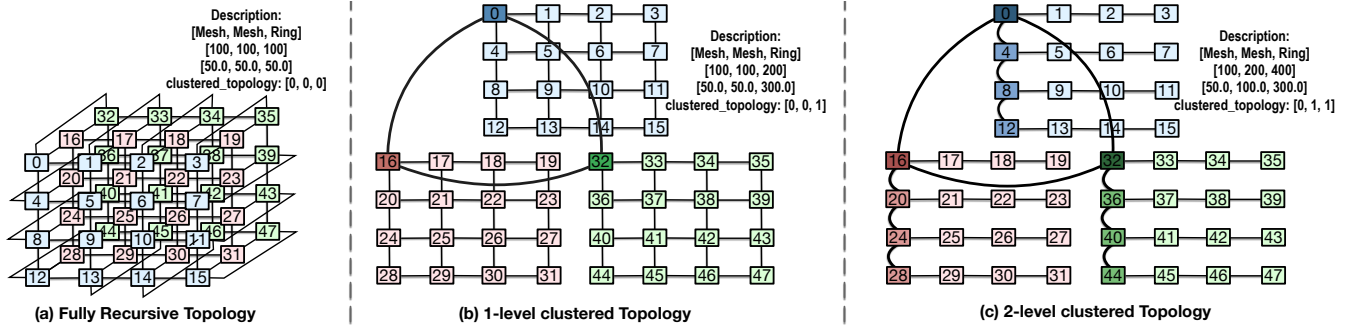


Figure 3. Topology structures supported by RAPID-LLM’s network backend.

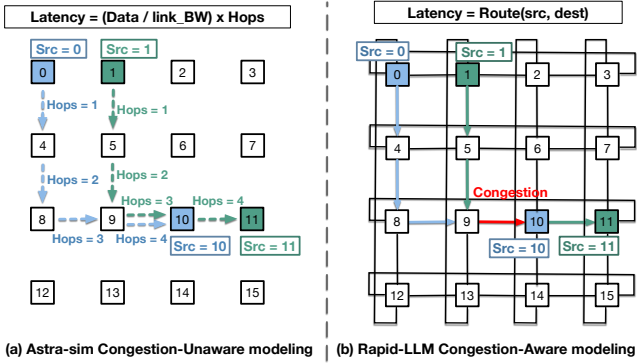


Figure 4. Congestion-aware modeling of multi-dimensional topologies in RAPID-LLM.

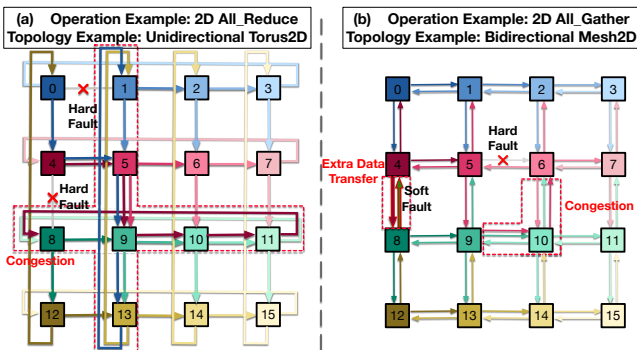


Figure 5. Examples of fault presence and RAPID-LLM’s routing to avoid hard faults, along with the resulting congestion on alternate links.

- **Flattened mode:** RAPID-LLM feeds the full per-GPU Chakra traces for an entire training or inference run directly into the network backend. Every compute and communication event, across all layers & micro-batches, appears in a single global timeline. This mode supports arbitrary network and parallelism configurations and is the most faithful representation of the

interaction between hybrid parallelism and network congestion.

- **Hierarchical mode:** RAPID-LLM decomposes the training or inference run into 3 hierarchical graphs (forward/backward pass of a single transformer layer and a pipeline graph across stages & microbatches) and feeds them to the network backend in sequence. This imposes some mild parallelism mapping constraints that are typical in modern deployments (TP/SP/CP must be in first network dimension, PP and DP must be in outer dimensions) and results in a slight loss of multi-dimensional congestion fidelity. However, it reduces the amount of computation and networking events fed to the backend considerably, significantly increasing execution speed and enabling scaling to thousands of GPUs.

5 Validation

This section evaluates how well RAPID-LLM predicts end-to-end time per training batch and inference step latency for representative LLM workloads.

5.1 Methodology

Reference sources. We use two sources of ground truth. (1) Published end-to-end runtimes for large-scale GPT training and Llama inference [17]. (2) Our own measurements for small-scale DDP training on a local 4x A100 80GB PCIe system.

Hardware configuration. We validate on two A100-based environments. Figures 6 and 7 use published references for A100 SXM-class systems, whose effective compute throughput and interconnect bandwidth exceed PCIe variants. Figure 8 uses A100 PCIe, which typically operates at a lower power limit and delivers lower sustained compute throughput than SXM. This is reflected in the hardware config used to run the tests. We fit a single network overlap, and train/inference memory and compute utilization correction factors to better represent runtimes across a variety of configurations.

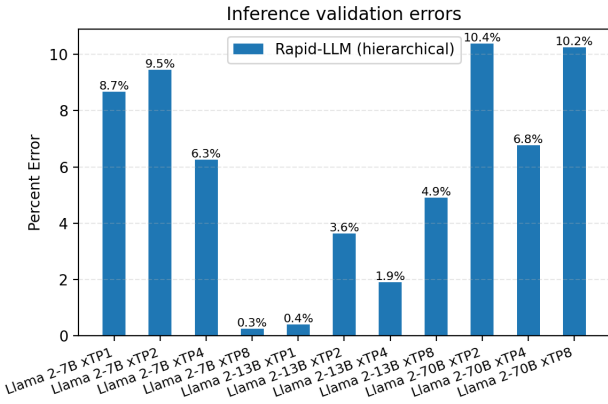


Figure 6. Predicted inference step latency for Llama2 (7B/13B/70B) under pure tensor parallelism across TP degrees, compared to published reference runtimes [17]. Error does not exceed 10.4%.

Execution mode. Unless stated otherwise, we use **Hierarchical** mode for the large-scale published cases to keep simulation cost practical at large GPU counts. For the 4-GPU microbenchmarks we run both flattened and hierarchical modes to quantify the approximation introduced by hierarchical decomposition.

5.2 Inference validation

Figure 6 evaluates inference step latency for Llama2-7B, 13B, and 70B under pure tensor parallelism (TP) across a range of TP degrees. These cases stress operator shape changes (prefill-like GEMMs versus decode-like skinny GEMMs) and model sensitivity to TP communication frequency. Across all evaluated cases, prediction error is at most 10.4% relative to published runtimes [17].

5.3 Training validation

Figure 7 reports percent error for end-to-end training time per batch across multiple GPT-scale configurations and parallelization choices on A100 clusters, compared to published references [17]. The plot separates two recomputation regimes. Full recomputation corresponds to checkpointing strategies that save memory by storing fewer activations and recomputing all required activations during backpropagation. Partial recomputation is more selective and recomputes only a subset of activations [6, 16]. Capturing recomputation matters because it changes both the total compute on the critical path and the degree of compute and communication overlap.

5.4 Small-scale DDP validation and mode comparison

Figure 8 validates DDP training using our own measurements for Llama2-7B on 4×A100 80GB PCIe under custom parallelism configurations. This setup exercises (i) network

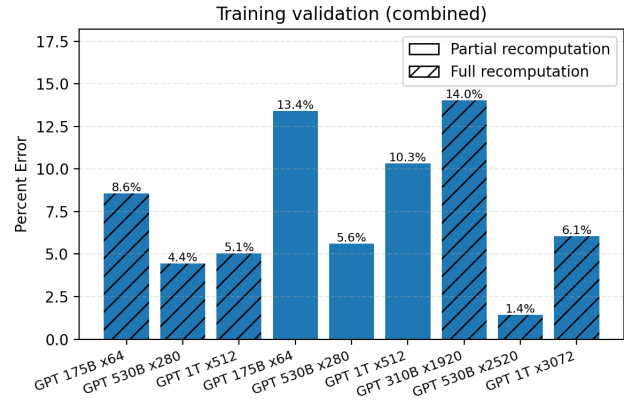


Figure 7. Predicted training time per batch across GPT-scale configurations on A100 clusters, compared to published reference runtimes [17]. We distinguish partial versus full activation recomputation regimes. Error does not exceed 14% across the cases evaluated.

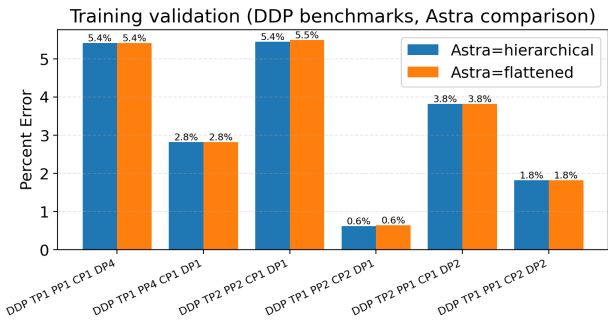


Figure 8. Predicted DDP training time per batch for Llama2-7B on 4×A100 PCIe, compared to our measurements. Flattened and hierarchical modes are near-identical (max difference $\approx 0.1\%$); overall error is within 5.5%.

derating under a small scale test (ii) small-scale communication behavior without calibrating to a specific cluster trace. We also compare flattened versus hierarchical execution modes; the two remain nearly identical on these runs (maximum difference $\approx 0.1\%$), while overall prediction error remains within 5.5%.

5.5 Network backend validation against ns-3

We validate the network backend by comparing it's predicted communication time against ns-3, a widely used discrete-event packet-level network simulator [28]. We focus on communication patterns induced by different parallelism axes, since these stress different collective and point-to-point behaviors. Figure 9 compares three backends: Astra-Sim (stock), RAPID-LLM's extended backend, and ns-3, across the topologies shown in the figure. The workload corresponds to the

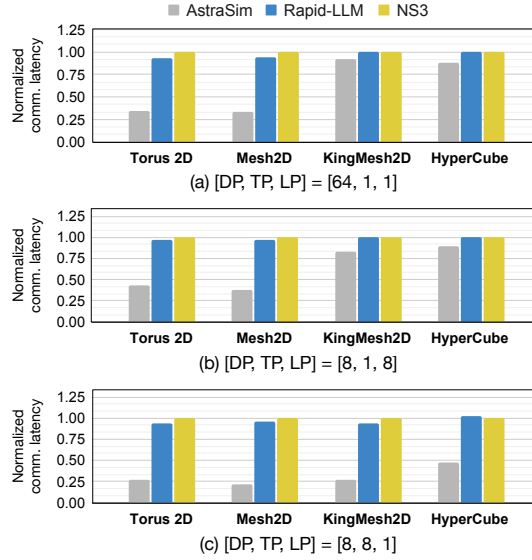


Figure 9. Network backend validation against Astra-Sim (stock) and ns-3 for three communication workloads corresponding to different parallelism patterns for Llama3.1-70B (sequence length 4096, batch size 128). RAPID-LLM stays within 8% of ns-3 across the shown topologies.

communication structure of Llama3.1-70B training on an A100 80GB-based system.

Across all tested cases, RAPID-LLM stays within 8% of ns-3. For congestion-free communication patterns such as pipeline-parallel point-to-point transfers, Astra-Sim (stock) and RAPID-LLM closely match each other, as expected. For cases with multi-flow contention, RAPID-LLM tracks ns-3 more closely due to explicit per-link queueing and multi-dimensional contention modeling. We use ns-3 only for small validation cases because packet-level simulation becomes expensive as network size and the number of concurrent flows increase. Furthermore, to keep execution time manageable, the reported runtime does not consider any compute nodes and only consists of the aggregated collectives that the training runs would exercise.

6 Case studies

RAPID-LLM targets questions that are hard to answer with trace replay or coarse layer-level models: sensitivity to link degradation, choosing hybrid-parallel configurations under concrete topologies, and comparing hypothetical GPU design points without re-profiling. This section presents three short studies that stress those capabilities.

6.1 Fault sensitivity under soft link degradation

We first study how single degraded links affect end-to-end training time. The setup is Llama3.1-70B training on 64 A100 80GB PCIe GPUs mapped onto a Torus2D + Ring fabric. We

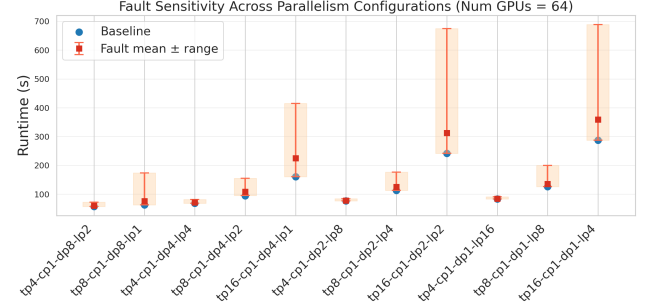


Figure 10. Fault sensitivity for Llama3.1-70B training on 64 A100 80GB SXM GPUs in a Torus2D (100GB/s/link, tp/cp) + Ring (25GB/s/link, dp/lp) topology. For each memory-feasible parallelism configuration, we inject single soft-link faults at multiple locations and report the resulting runtime degradation relative to the fault-free baseline.

enumerate a large set of memory-feasible hybrid-parallel configurations (DP/TP/PP/CP degrees and the implied communication patterns), then evaluate each configuration under many single-fault injections.

For this analysis we model *soft* faults only: a faulty link remains usable, but its effective bandwidth is reduced (equivalently, it incurs a retransmission or rate penalty). We implement this by applying a bandwidth derating factor to a single physical link in the instantiated topology and re-running the same communication schedule. Because the backend tracks per-link contention and queueing, a degraded link, especially in a higher dimension order can impact a large number of collectives and severely slow down runtime. We run a Monte Carlo simulation across many single fault iterations to gather representative results, assuming a Gaussian bandwidth derate of mean : 50%, std : 0.1. Figure 10 shows that fault impact depends strongly on the parallelism configuration and on fault location. Some configurations degrade sharply under a subset of fault placements because their dominant collectives or point-to-point transfers repeatedly traverse a small set of critical links. Other configurations are more robust because their traffic is lower or is spread more evenly across dimensions.

6.2 Exhaustive parallelism sweep on a fixed system

RAPID-LLM can also be used as a fast search tool over the hybrid-parallel design space for a given cluster. Figure 11 reports predicted Llama3.1-70B training time across a broad sweep of feasible configurations on the same 64-GPU system.

This sweep highlights a practical point: for a fixed model and hardware, the choice of parallelism degrees and mapping can change end-to-end time dramatically. The best configuration is shaped by the interaction between operator shapes (which set compute and memory behavior), the parallelism

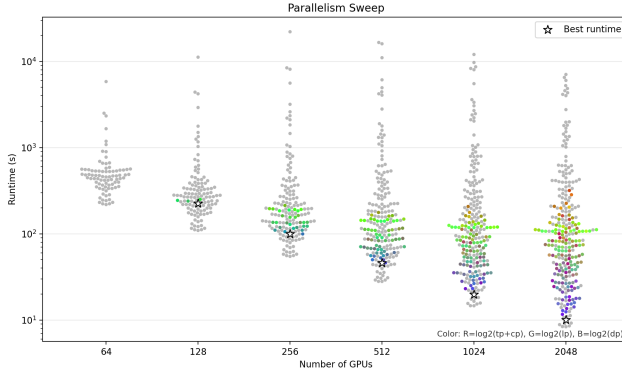


Figure 11. Predicted training time for Llama3.1-70B across a broad sweep of memory-feasible hybrid-parallel configurations on the target system.

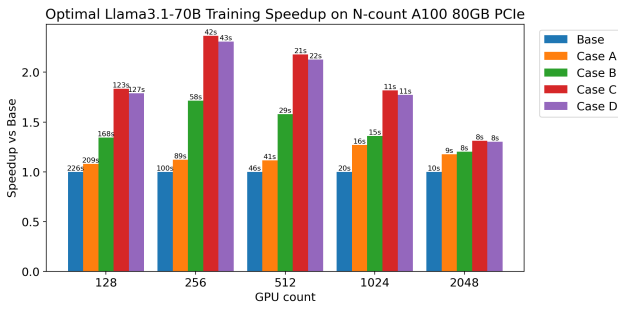


Figure 12. Training speedup vs. GPU hardware configuration (normalized to Base). Base: A100 80GB PCIe. Case A: A100 with stacked L2. Case B: A100 with 160GB 2.5D HBM. Case C: A100 with 3D stacked HBM (4× DRAM bandwidth). Case D: Case C with sustained 73% thermal-induced bandwidth throttle [14].

collective behavior (which determines communication volume and concurrency), and the topology and congestion behavior of the fabric. Because RAPID-LLM prunes memory-infeasible configurations and can evaluate candidate configurations quickly without a full training/inference run, it can serve as a front-end filter or tuner to select a configuration for a real system description without collecting traces.

6.3 GPU design variants and thermal throttling

Figure 12 uses RAPID-LLM as a “what-if” tool for GPU design variants while holding the model and parallelism configuration fixed. The baseline is an A100 80GB PCIe-like device. We then modify a small set of hardware-spec knobs that directly affect operator time: peak compute throughput, SRAM/L2 capacity and bandwidth, and HBM capacity and bandwidth. Because the frontend’s operator model is tile- and memory-hierarchy-aware, these changes propagate differently to different operators (for example, attention and

GEMMs versus bandwidth-dominated pointwise and reduction kernels), rather than acting as a single global scaling factor.

Case A increases the effective on-chip cache capacity by 2.5× by modeling a stacked L2 configuration. This primarily benefits GEMM reuse and FlashAttention tiles, reducing off-chip traffic and required memory bandwidth. Case B increases HBM capacity (160GB), which expands the space of memory-feasible training configurations and can reduce the need for aggressive activation recomputation, improving end-to-end runtime. Case C represents a 3D stacked HBM case, which is assumed to result in a 4× bandwidth [7] improvement.

Case D models a practical constraint for high-bandwidth HBM stacks: thermal limits can reduce sustained memory bandwidth via throttling. We implement this by applying a bandwidth derating factor (73% throttle[14]) to the HBM bandwidth parameter in the hardware specification. This shows how RAPID-LLM can be flexibly used to account for real-world hardware effects that are only measurable after deployment, such as thermal throttling.

7 Discussion & Conclusion

RAPID-LLM is built for the gap between two common extremes: high-fidelity trace replay that is tied to a specific deployment, and coarse analytical scaling models that cannot reflect operator shape, memory hierarchy behavior, or routing-dependent congestion. By generating hardware-aware operator-level Chakra traces from abstract LLM and hardware specifications, then executing them on an explicit multi-dimensional, congestion- and fault-aware network model, RAPID-LLM supports cluster-scale studies while remaining fast enough to sweep many design points.

RAPID-LLM provides a unified, scalable way to study end-to-end LLM training and inference performance under hybrid parallelism while keeping enough hardware and network detail to make predictions sensitive to memory hierarchy, congestion, and link degradation.

References

- [1] Mohammad Al-Fares, Alexander Loukissas, and Amin Vahdat. 2008. A scalable, commodity data center network architecture. *ACM SIGCOMM computer communication review* 38, 4 (2008), 63–74.
- [2] Reza Yazdani Aminabadi, Samyam Rajbhandari, Ammar Ahmad Awan, Cheng Li, Du Li, Elton Zheng, Olatunji Ruwase, Shaden Smith, Minjia Zhang, Jeff Rasley, and Yuxiong He. 2022. DeepSpeed-Inference: Enabling Efficient Inference of Transformer Models at Unprecedented Scale. In *Proceedings of the International Conference for High Performance Computing, Networking, Storage and Analysis (SC ’22)*. IEEE Press, Article 46, 15 pages. doi:10.5555/3571885.3571946
- [3] Ali Bakhoda, George L. Yuan, Wilson W. L. Fung, Henry Wong, and Tor M. Aamodt. 2009. Analyzing CUDA Workloads Using a Detailed GPU Simulator. In *Proceedings of the IEEE International Symposium on Performance Analysis of Systems and Software (ISPASS)*. IEEE Computer Society, 163–174. doi:10.1109/ISPASS.2009.4919648

[4] Jaehong Cho, Minsu Kim, Hyunmin Choi, Guseul Heo, and Jongse Park. 2024. LLMervingSim: A HW/SW Co-Simulation Infrastructure for LLM Inference Serving at Scale. In *Proceedings of the IEEE International Symposium on Workload Characterization (IISWC)*. IEEE, 15–29. doi:10.1109/IISWC63097.2024.00012

[5] William James Dally and Brian Patrick Towles. 2004. *Principles and practices of interconnection networks*. Elsevier.

[6] Tri Dao, Daniel Y. Fu, Stefano Ermon, Atri Rudra, and Christopher Re. 2022. FLASHATTENTION: fast and memory-efficient exact attention with IO-awareness. In *Proceedings of the 36th International Conference on Neural Information Processing Systems* (New Orleans, LA, USA) (NIPS '22). Curran Associates Inc., Red Hook, NY, USA, Article 1189, 16 pages.

[7] Debendra Das Sharma, Gerald Pasdast, Sathya Tiagaraj, and Kemal Aygün. 2024. High-performance, power-efficient three-dimensional system-in-package designs with universal chiplet interconnect express. *Nature Electronics* 7, 3 (March 2024), 244–254. doi:10.1038/s41928-024-01126-y

[8] Abhimanyu Dubey, Abhinav Jauhri, Abhinav Pandey, Abhishek Kadian, Ahmad Al-Dahle, Aiesha Letman, Akhil Mathur, Alan Schelten, Amy Yang, Angela Fan, et al. 2024. The llama 3 herd of models. *arXiv e-prints* (2024), arXiv-2407.

[9] Phillipa Gill, Navendu Jain, and Nachiappan Nagappan. 2011. Understanding Network Failures in Data Centers: Measurement, Analysis, and Implications. In *Proceedings of the ACM SIGCOMM 2011 Conference (SIGCOMM '11)*. ACM, 350–361. doi:10.1145/2018436.2018477

[10] Haryadi S. Gunawi, Riza O. Suminto, Russell Sears, Casey Golligher, Swaminathan Sundararaman, Xing Lin, Tim Emami, Weiguang Sheng, Nematollah Bidokhti, Caitie McCaffrey, Gary Grider, Parks M. Fields, Kevin Harms, Robert B. Ross, Andree Jacobson, Robert Ricci, Kirk Webb, Peter Alvaro, H. Birali Runesha, Mingzhe Hao, and Huaicheng Li. 2018. Fail-Slow at Scale: Evidence of Hardware Performance Faults in Large Production Systems. In *16th USENIX Conference on File and Storage Technologies (FAST '18)*. USENIX Association, 1–14. <https://www.usenix.org/conference/fast18/presentation/gunawi>

[11] Hyungkyu Ham, Wonhyuk Yang, Yunseon Shin, Okkyun Woo, Guseul Heo, Sangyeop Lee, Jongse Park, and Gwangsun Kim. 2024. ONNXIM: A Fast, Cycle-Level Multi-Core NPU Simulator. *IEEE Computer Architecture Letters* 23, 2 (2024), 219–222. doi:10.1109/LCA.2024.3484648

[12] Peng Huang, Chuanxiong Guo, Lidong Zhou, Jacob R. Lorch, Yingnong Dang, Murali Chintalapati, and Randolph Yao. 2017. Gray Failure: The Achilles' Heel of Cloud-Scale Systems. In *Proceedings of the 16th Workshop on Hot Topics in Operating Systems (HotOS '17)*. ACM, 150–155. doi:10.1145/3102980.3103005

[13] Yaping Huang, Youlong Cheng, Ankur Bapna, Orhan Firat, Dehao Chen, Mia Chen, HyoukJoong Lee, Jiquan Ngiam, Quoc V Le, Yonghui Wu, et al. 2019. Gpipe: Efficient training of giant neural networks using pipeline parallelism. *Advances in neural information processing systems* 32 (2019).

[14] George Karfakis, Myriam Bouzidi, Yunhyeok Im, Alexander Graening, Suresh K. Sitaraman, and Puneet Gupta. 2025. Optimizing Thermal Performance in 2.5D Systems Using Embedded Isolators. *IEEE Journal on Emerging and Selected Topics in Circuits and Systems* 15, 3 (2025), 458–468. doi:10.1109/JETCAS.2025.3595909

[15] Mahmoud Khairy, Zhesheng Shen, Tor M. Aamodt, and Timothy G. Rogers. 2020. Accel-Sim: An Extensible Simulation Framework for Validated GPU Modeling. In *Proceedings of the ACM/IEEE Annual International Symposium on Computer Architecture (ISCA)*. IEEE, 473–486. doi:10.1109/ISCA45697.2020.00047

[16] Vijay Anand Korthikanti, Jared Casper, Sangkug Lym, Lawrence McAfee, Michael Andersch, Mohammad Shoeybi, and Bryan Catanzaro. 2023. Reducing activation recomputation in large transformer models. *Proceedings of Machine Learning and Systems* 5 (2023), 341–353.

[17] Joyjit Kundu, Wenzhe Guo, Ali BanaGozar, Udari De Alwis, Sourav Sengupta, Puneet Gupta, and Arindam Mallik. 2024. Performance Modeling and Workload Analysis of Distributed Large Language Model Training and Inference. In *2024 IEEE International Symposium on Workload Characterization (IISWC)*. 57–67. doi:10.1109/IISWC63097.2024.00015

[18] Woosuk Kwon, Zhuohan Li, Siyuan Zhuang, Ying Sheng, Lianmin Zheng, Cody Hao Yu, Joseph E. Gonzalez, Hao Zhang, and Ion Stoica. 2023. Efficient Memory Management for Large Language Model Serving with PagedAttention. In *Proceedings of the 29th Symposium on Operating Systems Principles (SOSP '23)*. ACM, 611–626. doi:10.1145/3600006.3613165

[19] Ang Li, Shuaiwen Leon Song, Jieyang Chen, Jiajia Li, Xu Liu, Nathan R. Tallent, and Kevin J. Barker. 2020. Evaluating Modern GPU Interconnect: PCIe, NVLink, NV-SLI, NVSwitch and GPUDirect. *IEEE Transactions on Parallel and Distributed Systems* 31, 1 (2020), 94–110. doi:10.1109/TPDS.2019.2928289

[20] Hao Liu, Matei Zaharia, and Pieter Abbeel. 2023. Ring attention with blockwise transformers for near-infinite context. *arXiv preprint arXiv:2310.01889* (2023).

[21] Shanghai Man, Joongun Park, Hanjiang Wu, Huan Xu, Srinivas Sridharan, and Tushar Krishna. 2025. STAGE: A Symbolic Tensor grAph GEnerator for distributed AI system co-design. *arXiv:2511.10480* [cs.DC] doi:10.48550/arXiv.2511.10480

[22] NVIDIA Corporation. 2025. *NVIDIA Ethernet Networking*. <https://www.nvidia.com/en-us/networking/products/ethernet/> Accessed: Dec. 2, 2025.

[23] NVIDIA Corporation. 2025. *NVIDIA InfiniBand Networking*. <https://www.nvidia.com/en-us/networking/products/infiniband/> Accessed: Dec. 2, 2025.

[24] NVIDIA Corporation. 2025. *NVIDIA NVLink*. <https://www.nvidia.com/en-us/data-center/nvlink/> Accessed: Dec. 2, 2025.

[25] SAPTADEEP PAL and PUNEET GUPTA. 2023. DeepFlow: A Cross-Stack Pathfinding Framework for Distributed AI Systems. (2023).

[26] Huwan Peng, Scott Davidson, C.-J. Richard Shi, and Michael B. Taylor. 2025. ReaLLM: A Trace-Driven Framework for Rapid Simulation of Large-Scale LLM Inference. In *Proceedings of the IEEE International Conference on Application-specific Systems, Architectures and Processors (ASAP)*. IEEE, 85–92. doi:10.1109/ASAP65064.2025.00022

[27] Samyam Rajbhandari, Jeff Rasley, Olatunji Ruwase, and Yuxiong He. 2020. ZeRO: Memory Optimizations Toward Training Trillion Parameter Models. In *Proceedings of the International Conference for High Performance Computing, Networking, Storage and Analysis (SC '20)*. IEEE Press, Article 20, 16 pages. doi:10.5555/3433701.3433727

[28] George F. Riley and Thomas R. Henderson. 2010. The ns-3 Network Simulator. In *Modeling and Tools for Network Simulation*, Klaus Wehrle, James Gross, and Mesut Güneş (Eds.). Springer, Berlin, Heidelberg, 15–34. doi:10.1007/978-3-642-12331-3_2

[29] Adel Sefiane, Alireza Farshin, and Marios Kogias. 2025. MLSynth: Towards Synthetic ML Traces. In *Proceedings of the 2nd Workshop on Networks for AI Computing (NAIC '25)*. ACM, 98–104. doi:10.1145/3748273.3749211

[30] Mohammad Shoeybi, Mostofa Patwary, Raul Puri, Patrick LeGresley, Jared Casper, and Bryan Catanzaro. 2019. Megatron-lm: Training multi-billion parameter language models using model parallelism. *arXiv preprint arXiv:1909.08053* (2019).

[31] Srinivas Sridharan, Taekyung Heo, Louis Feng, Zhaodong Wang, Matt Bergeron, Wenyin Fu, Shengbao Zheng, Brian Coutinho, Saeed Rashidi, Shanghai Man, and Tushar Krishna. 2023. Chakra: Advancing performance benchmarking and co-design using standardized execution traces. *arXiv [cs.LG]* (May 2023).

[32] Xizheng Wang, Qingxu Li, Yichi Xu, Gang Lu, Dan Li, Li Chen, Heyang Zhou, Linkang Zheng, Sen Zhang, Yikai Zhu, Yang Liu, Pengcheng Zhang, Kun Qian, Kunling He, Jiaqi Gao, Ennan Zhai, Dennis Cai,

and Binzhang Fu. 2025. SimAI: Unifying Architecture Design and Performance Tuning for Large-Scale Large Language Model Training with Scalability and Precision. In *Proceedings of the USENIX Symposium on Networked Systems Design and Implementation (NSDI)*. USENIX Association, 541–558.

[33] William Won, Taekyung Heo, Saeed Rashidi, Srinivas Sridharan, Sudarshan Srinivasan, and Tushar Krishna. 2023. ASTRA-sim2.0: Modeling Hierarchical Networks and Disaggregated Systems for Large-model Training at Scale. In *2023 IEEE International Symposium on Performance Analysis of Systems and Software (IPASS)*. 283–294. doi:10.1109/IPASS57527.2023.00035

[34] Hengrui Zhang, August Ning, Rohan Baskar Prabhakar, and David Wentzlaff. 2024. LLMCompass: Enabling Efficient Hardware Design for Large Language Model Inference. In *Proceedings of the ACM/IEEE Annual International Symposium on Computer Architecture (ISCA)*. IEEE, 1080–1096. doi:10.1109/ISCA59077.2024.00082